



Colombo, A., Di Bernardo, M., Fossas, E., & Jeffrey, MR. (2010).  
Teixeira singularities in 3D switched feedback control systems.  
*Systems and Control Letters*, 59(10), 615 - 622.  
<https://doi.org/10.1016/j.sysconle.2010.07.006>

Early version, also known as pre-print

Link to published version (if available):  
[10.1016/j.sysconle.2010.07.006](https://doi.org/10.1016/j.sysconle.2010.07.006)

[Link to publication record in Explore Bristol Research](#)  
PDF-document

## University of Bristol - Explore Bristol Research

### General rights

This document is made available in accordance with publisher policies. Please cite only the published version using the reference above. Full terms of use are available:  
<http://www.bristol.ac.uk/red/research-policy/pure/user-guides/ebr-terms/>

# Teixeira singularities in 3D switched feedback control systems.

A Colombo<sup>a</sup>, M di Bernardo<sup>b</sup>, E Fossas<sup>c</sup>, M R Jeffrey<sup>d</sup>

March 16, 2010

## Abstract

This paper is concerned with the analysis of a singularity that can occur in three-dimensional discontinuous feedback control systems. The singularity is the two-fold – a tangency of orbits to both sides of a switching manifold. Particular attention is placed on the Teixeira singularity, which previous literature suggests as a mechanism for dynamical transitions in this class of systems. We show that such a singularity cannot occur in classical single-input single-output systems in the Lur’e form. It is, however, a potentially dangerous phenomenon in multiple-input multiple-output switched control systems. The theoretical derivation is illustrated by means of a representative example.

keywords: feedback, Filippov, Lur’e, piecewise smooth, two-fold

## 1 Introduction and Background

Hybrid and switched models are being increasingly used in applications to describe a large variety of physical devices. Examples include mechanical systems with friction and backlash, electrical and electronic circuits, walking and hopping robots and, more recently, biological and neural systems [19, 20, 2, 3, 4, 14, 21, 8, 7, 9, 26, 5, 10, 15, 1, 6]. Many of these systems can be described by sets of piecewise smooth ordinary differential equations (ODEs) whose phase space is partitioned, by a set of switching manifolds, in different regions each associated to a different functional form of the system vector field. Much research attention has been focussed on the analysis of piecewise smooth dynamical systems (see for example [13, 22, 11]). These systems can exhibit several interesting phenomena, including sliding motion, which occurs in a region of

---

<sup>a</sup> Corresponding author. Department of Electronics and Information, Politecnico di Milano, Via Ponzio 34/5, 20133 Milan, Italy (alessandro.colombo@polimi.it).

<sup>b</sup> Department of Systems and Computer Science, University of Naples Federico II, Via Claudio 21, 80125 Napoli, Italy, and Applied Nonlinear Mathematics Group, Department of Engineering Mathematics, University of Bristol, Queen’s Building, University Walk, Bristol BS8 1TR, UK (m.dibernardo@unina.it).

<sup>c</sup> Institute of Industrial and Control Engineering and Department of Automatic Control, Universitat Politècnica de Catalunya, Avda. Diagonal, 647 pl. 11. 08028 Barcelona, Spain (enric.fossas@upc.edu).

<sup>d</sup> Applied Nonlinear Mathematics Group, Department of Engineering Mathematics, University of Bristol, Queen’s Building, University Walk, Bristol BS8 1TR, UK (mike.jeffrey@bristol.ac.uk).

the switching manifold termed the sliding region, where the system vector field points towards the manifold from both sides. If a trajectory intersects the sliding region, say  $\Sigma^s$ , it is then constrained to evolve on it until reaching its boundary  $\partial\Sigma^s$ . Such a boundary occurs where the vector field is tangent to the switching manifold on at least one side. One can thus distinguish between two boundaries, depending on which side of the switching manifold the vector field is tangent to. In many systems of interest in applications, such boundaries do not intersect in the interesting region of phase space. For example, in three-dimensional relay control systems or friction oscillators, the boundaries have been shown to be parallel lines in the switching manifold.

In their pioneering work on piecewise smooth systems, Teixeira and, independently, Filippov, have proposed that, if the boundaries of the sliding region intersect transversely at a point called a two-fold, this can have a dramatic effect on the system dynamics [23, 13, 24]. For particular configurations of the vector field, dynamics in a neighbourhood of such points can be structurally unstable, and the dynamics around these points can be rather intricate. To date we are not aware of the two-fold having been observed in a control system, however until recently little was known about even the qualitative dynamics around the singularity. Recently [18] have shown that a particular occurrence of the two-fold, called the Teixeira singularity, may exist in two forms (see Figure 1). In one case, shown in the left of Figure 1, trajectories flow safely past the

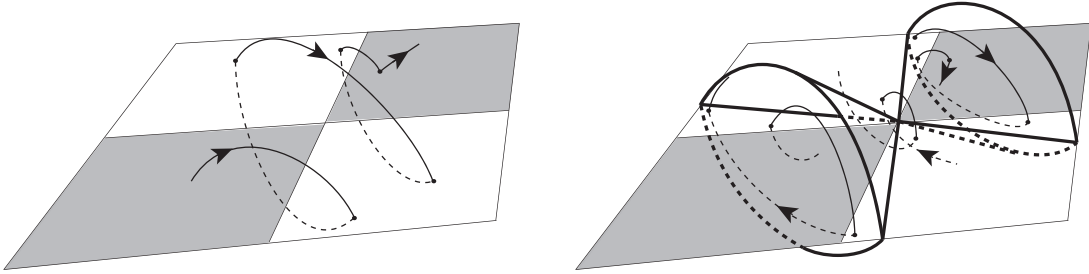


Figure 1: Dynamics around the Teixeira singularity. Left: the benign case, orbits spiral around from the escaping to sliding region. Right: the diabolical case, a double cone creased at the switching manifold delimits regions of attraction (surrounding the sliding region), of repulsion (surrounding the escaping region), and of spiralling flow (outside the double cone).

singularity, and therefore it could certainly be missed. In a potentially more dangerous form (right in Figure 1), the singularity sits at the apex of a pair of creased cones – a ‘nonsmooth diabolos’ – attracting orbits within one and repelling them within the other, and trajectories may reach the singularity via the sliding region, where lack of uniqueness at the singularity provides the conditions for a nondeterministic form of chaos [12]. Between the two cases is a bifurcation associated with the birth of limit cycles.

Now, one of the most notable applications of hybrid and switched systems is the design of controllers based on the use of switching actions as, for instance, variable structure controllers [27]. For example, it has been suggested in [28, 16] that switched state feedback controllers, or switched PID controllers can be used effectively to achieve some desired control objective in the presence of changes in the operating conditions, noise or unmodelled dynamics. Therefore, an open problem is to assess whether Teixeira singularities are present in the closed-loop systems

under a switched control action as this aspect seems to have been neglected in many of the classical books and papers on the topic. The analysis can have two possible outcomes: either Teixeira singularities are not possible or such phenomena can indeed occur in a switched control system. In the latter case, rigorous conditions for their occurrence (or avoidance) should be given together with a classification of the possible dynamical scenarios they organise.

This suggests that a gap exists in the literature on the dynamics of switched control systems, which this paper aims to fill by studying the occurrence of Teixeira singularities in three-dimensional switched output- and state-feedback controllers. In particular, starting from systems in the classical Lur'e form, we then investigate the case of more general switched multi-input multi-output controllers. In so doing, we give analytical conditions for the occurrence of Teixeira singularities and the classification of the associated dynamics they induce. By using a representative example, we validate the theoretical derivation via appropriate numerical simulations.

The rest of the paper is outlined as follows: in Section 2, we introduce the Teixeira singularity and give algebraic conditions for its occurrence. In Section 3, we classify the dynamic regimes that can be found around this singularity and then, in Section 4, we investigate how this singularity can take place, or be avoided, in different control schemes. Finally, in Section 5 we discuss some examples.

## 2 The two-fold singularity

We consider a three-dimensional piecewise smooth dynamical system of the form

$$\dot{x} = \begin{cases} F^+(x), & \sigma(x) > 0, \\ F^-(x), & \sigma(x) < 0, \end{cases} \quad (1)$$

where  $x \in \mathbb{R}^3$  is the state vector,  $F^\pm(x) : \mathbb{R}^3 \mapsto \mathbb{R}^3$  are the system vector fields and  $\sigma(x) : \mathbb{R}^3 \mapsto \mathbb{R}$  is the scalar function defining the *switching manifold*,  $\Sigma$ , by the condition

$$\Sigma := \{x \in \mathbb{R}^3 : \sigma(x) = 0\}.$$

Solutions of (1) are to be intended in the sense of Filippov's differential inclusions, hence, as we detail later on, forward or backward-time uniqueness of solutions is not granted in certain regions of the state space.

Following [23, 24, 25], a point  $\hat{x} \in \mathbb{R}^3$  is said to be a *two-fold singularity* of system (1) if it is a point where  $\Sigma$  is smooth and the flows of the two vector fields  $F^+(x)$  and  $F^-(x)$  are tangent to the switching manifold at  $x = \hat{x}$ . From now on, all functions of  $x$  evaluated at  $\hat{x}$  are written with the hat symbol and without argument. Specifically we give the following definition.

**Definition 1** *A point  $\hat{x}$  is a two-fold singularity if*

$$\dot{\hat{\sigma}} = \hat{\sigma}_x \hat{F}^+ = \hat{\sigma}_x \hat{F}^- = 0. \quad (2)$$

*Moreover, the following two nondegeneracy conditions, are satisfied:*

1. The curves along which the flows of the two vector fields are tangent to the switching manifold intersect transversely. That is

$$\det(T) \neq 0 \quad (3)$$

where

$$T = \begin{pmatrix} (\hat{\sigma}_x \hat{F}^+)_x \\ (\hat{\sigma}_x \hat{F}^-)_x \\ \hat{\sigma}_x \end{pmatrix}.$$

Note that  $(\hat{\sigma}_x \hat{F})_x = \hat{\sigma}_x \hat{F}_x + \hat{\sigma}_{xx} F$ , where  $F_x(x)$  is the Jacobian matrix of  $F(x)$ , and  $\sigma_{xx}(x)$  is the Hessian matrix of  $\sigma(x)$  that vanishes when  $\Sigma$  is flat.

2. The vector fields are quadratically tangent to the switching manifold near the singularity, that is  $\ddot{\sigma} = (\hat{\sigma}_x \hat{F}^\pm)_x \hat{F}^\pm \neq 0$ .

The first condition is illustrated in Figure 2 where, for simplicity,  $\sigma(x)$  and  $\sigma_x(x)F^\pm(x)$  are presumed to be affine functions of  $x$ . If  $T$  is singular then either the nullclines  $\sigma_x(x)F^\pm(x) = 0$  are coplanar or their intersection with  $\Sigma$  is not a unique point. If  $T$  is nonsingular then the switching plane  $\sigma(x) = 0$ , and the nullcline planes  $\sigma_x(x)F^+(x) = 0$  and  $\sigma_x(x)F^-(x) = 0$ , are in a generic position relative to each other, meaning that none are coplanar and that their three pairwise lines of intersection cross at a unique point: the two-fold singularity.

An alternative interpretation is possible by noticing that, when  $\hat{\sigma}_{xx} = 0$ , we can rearrange the determinant into the form

$$\det(T) = \det(\hat{\sigma}_x \hat{P}_x, \hat{\sigma}_x \hat{Q}_x, \hat{\sigma}_x) \quad (4)$$

where  $P(x) = (F^+(x) + F^-(x))/2$  is the average of the vector fields at the switching manifold and  $Q(x) = F^+(x) - F^-(x)$  is the size of the correction applied there. The singularity condition states that the rotation axis  $\hat{\sigma}_x \hat{P}_x \times \hat{\sigma}_x \hat{Q}_x$  is non-vanishing and does not lie in the switching manifold.

The second condition distinguishes between three qualitatively different singularities as illustrated in Figure 3:

1. **The Teixeira singularity**, where  $(\hat{\sigma}_x \hat{F}^+)_x \hat{F}^+ < 0 < (\hat{\sigma}_x \hat{F}^-)_x \hat{F}^-$ .
2. **The visible two-fold**, where  $(\hat{\sigma}_x \hat{F}^-)_x \hat{F}^- < 0 < (\hat{\sigma}_x \hat{F}^+)_x \hat{F}^+$ .
3. **The visible-invisible two-fold**, where  $(\hat{\sigma}_x \hat{F}^+)_x \hat{F}^+ (\hat{\sigma}_x \hat{F}^-)_x \hat{F}^- > 0$ .

In what follows, we focus our investigation on the Teixeira singularity in generic three-dimensional switched control systems consisting of a linear forward path and a switching feedback action.

Note that, in general, the switching manifold around a two-fold singularity is divided into four regions: one where the vector field points towards the manifold from both sides, named the sliding region ( $\Sigma^s$ ); one where the vector field points away from the manifold from both sides,

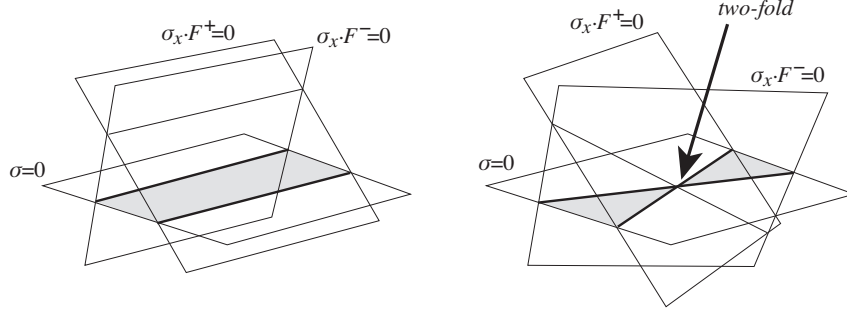


Figure 2: Critical surfaces and the two-fold. The switching manifold is  $\sigma(x) = 0$ , and the normal components of the vector fields vanish where  $\sigma_x F^+ = 0$  or  $\sigma_x F^- = 0$ . For simplicity we show the case when  $\sigma_x, \sigma_x F_x^+, \sigma_x F_x^-$ , do not depend on  $x$ , and  $\sigma_{xx} = 0$ , so the surfaces are planar. Left: no singularity when  $\det(\sigma_x F_x^+, \sigma_x F_x^-, \sigma_x) = 0$  because the pairwise intersections of the planes do not cross. Right: in the generic case  $\det(\sigma_x F_x^+, \sigma_x F_x^-, \sigma_x) \neq 0$  the three planes intersect to form a two-fold singularity.

named the escaping region ( $\Sigma^e$ ); and two where the vector field normal component to the manifold has the same direction on the two sides, named the crossing regions ( $\Sigma^c$ ). In the particular case of a Teixeira singularity, (Figure 3-1) the curvature of the vector fields on the two sides of the switching manifold wraps orbits around the singularity, generating intricate dynamics that depend on the relative direction of the vector fields at the singularity, as we explain in the next section.

Ideal sliding dynamics can be assumed to apply in the sliding and escaping regions, where  $\sigma(x) = 0$  and  $\sigma_x F^+(x)\sigma_x F^-(x) < 0$ . Sliding orbits herald a loss of uniqueness of solutions. In the sliding region where  $\sigma_x F^+(x) < 0 < \sigma_x F^-(x) < 0$  trajectories from  $F^\pm(x)$  are attracted to  $\Sigma$  in finite time, and are non-unique in reverse time. In the escaping region where  $\sigma_x F^-(x) < 0 < \sigma_x F^+(x) < 0$  trajectories from  $F^\pm(x)$  are repelled away from  $\Sigma$  in finite time, and are non-unique in forward time. Sliding orbits, confined to the open regions satisfying these conditions, are solutions of

$$\dot{x} = \mathcal{F}(x) := \frac{\sigma_x F^-(x)F^+(x) - \sigma_x F^+(x)F^-(x)}{\sigma_x(F^-(x) - F^+(x))} \quad (5)$$

$$:= \frac{1}{\sigma_x(F^-(x) - F^+(x))} \tilde{\mathcal{F}}(x). \quad (6)$$

The normalised sliding vector field  $\tilde{\mathcal{F}}(x)$  is obtained by multiplying  $\mathcal{F}(x)$  by the scalar function  $\sigma_x(F^-(x) - F^+(x))$ , which goes to zero at the singularity. Hence the dynamics of  $\mathcal{F}(x)$  and  $\tilde{\mathcal{F}}(x)$  are equivalent except at the singularity, where  $\tilde{\mathcal{F}}(x)$  has an equilibrium due to the normalisation. As a consequence, orbits that reach the singularity or depart from it asymptotically in  $\tilde{\mathcal{F}}(x)$ , do so in *finite* time in  $\mathcal{F}(x)$ . Additionally, orbits of  $\tilde{\mathcal{F}}(x)$  and  $\mathcal{F}(x)$  flow in opposite direction in  $\Sigma^e$ , where  $\sigma_x(F^-(x) - F^+(x))$  is negative. Keeping in mind these important differences, sliding dynamics around the singularity can be effectively analysed by studying the orbits of  $\tilde{\mathcal{F}}(x)$ .

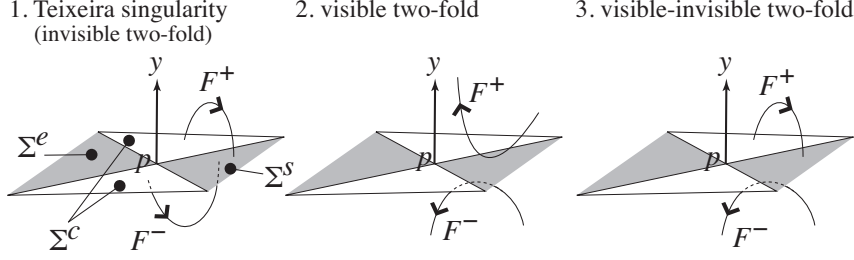


Figure 3: Types of two-fold: 1. the Teixeira singularity, 2. the visible two-fold, and 3. the visible-invisible two-fold. Typical orbits of the vector fields  $F^\pm$  are shown. Regions are labelled as in the text:  $\Sigma^c$  crossing regions,  $\Sigma^s$  sliding region,  $\Sigma^e$  escaping region.

### 3 Classification of the dynamics

Without loss of generality we assume  $\sigma(x)$  to be a linear function of  $x$  in the region of interest, so that  $\sigma_x$  does not depend on  $x$  and  $\sigma_{xx} = 0$  (this is achieved with a suitable change of variables near any smooth portion of the switching manifold). [18] classified the dynamics in the neighbourhood of the Teixeira-singularity as follows. Let the singularity be at  $\hat{x}$ . Define the two quantities  $v$  and  $w$  as

$$v = -\frac{\sigma_x \hat{F}_x^- \hat{F}^+}{\sigma_x \hat{F}_x^+ \hat{F}^+} \quad w = -\frac{\sigma_x \hat{F}_x^+ \hat{F}^-}{\sigma_x \hat{F}_x^- \hat{F}^-}. \quad (7)$$

The quantity  $v$  measures the component of  $\hat{F}^+$  that is normal to the tangency line of  $F^-$ , divided by the component that is normal to the tangency line of  $F^+$ , while  $w$  measures the component of  $\hat{F}^-$  that is normal to the tangency line of  $F^+$ , divided by the component normal to the tangency line of  $F^-$ . These definitions greatly simplify the analysis, since  $v$  and  $w$  go to zero when  $\hat{F}^\pm$  is tangent to the tangency line of  $F^\mp$ , while their product goes to unity when  $\hat{F}^+$  and  $\hat{F}^-$  have the same direction. In this case one can either have  $v, w < 0$ , in which case  $\hat{F}^+$  and  $\hat{F}^-$  have opposite orientations, or  $v, w > 0$ , when they have same orientation. Notice that the denominators are bounded away from zero by nondegeneracy condition 2 in Definition 1.

Then the dynamics, as described below, depend on the quantities:

$$vw - 1 = -\frac{\det \begin{pmatrix} \sigma_x \hat{F}_x^+ \hat{F}^+ & \sigma_x \hat{F}_x^- \hat{F}^+ \\ \sigma_x \hat{F}_x^+ \hat{F}^- & \sigma_x \hat{F}_x^- \hat{F}^- \end{pmatrix}}{\sigma_x \hat{F}_x^+ \hat{F}^+ \sigma_x \hat{F}_x^- \hat{F}^-} \quad (8)$$

where  $\sigma_x \hat{F}_x^+ \hat{F}^+ = (\sigma_x \hat{F}^+)_x \hat{F}^+ < 0$  and  $\sigma_x \hat{F}_x^- \hat{F}^- = (\sigma_x \hat{F}^-)_x \hat{F}^- > 0$ , so

$$\text{sign } v = \text{sign}(\sigma_x \hat{F}_x^- \hat{F}^+) \quad (9)$$

$$\text{sign } w = -\text{sign}(\sigma_x \hat{F}_x^+ \hat{F}^-) \quad (10)$$

$$\text{sign}(vw - 1) = \text{sign} \left( \det \begin{pmatrix} \sigma_x \hat{F}_x^+ \hat{F}^+ & \sigma_x \hat{F}_x^- \hat{F}^+ \\ \sigma_x \hat{F}_x^+ \hat{F}^- & \sigma_x \hat{F}_x^- \hat{F}^- \end{pmatrix} \right) \quad (11)$$

Let a maximal orbit describe the concatenation of all segments of a single trajectory that lie above, below, or on the switching manifold, including intersection points where the orbit crosses or begins to slide. Orbits in the neighbourhood of the Teixeira singularity then satisfy the following:

- (i) If  $vw > 1$  and  $v, w < 0$ : any maximal orbit crosses the switching manifold an infinite number of times. There exist a pair of invariant surfaces that meet at the singularity. Additionally, orbits in the sliding region near the singularity reach it in finite time.
- (ii) Otherwise any orbit may only cross the switching manifold a finite number of times. Let  $N$  be the number of times a maximal orbit may cross the switching manifold :  $N \leq 1$  if  $v > 0$  and/or  $w > 0$ ,  $N \geq 1$  if  $0 < vw < 1$  and  $v, w < 0$ . Orbits in the sliding region near the singularity are repelled from it.

A bifurcation occurs when  $vw = 1$  with  $v, w < 0$ . A limit cycle is born from the singularity at the bifurcation, as it will be illustrated in the example section (for a detailed proof of this statement see [18]). For  $vw < 1$  the singularity is a saddlepoint of  $\tilde{\mathcal{F}}(x)$ , with its unstable manifold in the sliding region. For  $vw > 1$  the singularity is a node of  $\tilde{\mathcal{F}}(x)$ , which is repelling if  $v, w > 0$  and attracting if  $v, w < 0$ . Hence,  $vw > 1$  with  $v, w < 0$  is the only case where orbits in the sliding region are attracted toward the singularity.

## 4 Switched feedback control system

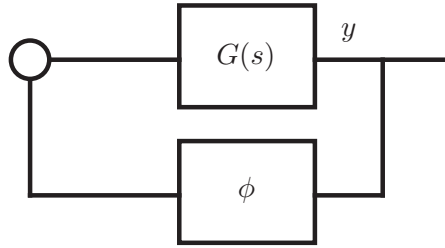


Figure 4: Lur'e system block diagram

The feedback control system of interest is sketched in Figure 4. It is a three-dimensional system with  $m$  inputs and  $p$  outputs consisting of a linear forward path and a switched nonlinear feedback. In the state-space domain, the linear part can be described as

$$\begin{aligned} \dot{x} &= Ax + Bu \\ y &= Cx, \end{aligned} \tag{12}$$

where  $x \in \mathbb{R}^3$ ,  $u \in \mathbb{R}^m$ ,  $y \in \mathbb{R}^p$ ,  $A \in \mathbb{R}^{3 \times 3}$ ,  $B \in \mathbb{R}^{3 \times m}$ ,  $C \in \mathbb{R}^{p \times 3}$ .



The feedback action is described by  $u = -\phi(y)$  where  $\phi : \mathbb{R}^p \mapsto \mathbb{R}^m$  is assumed to be a piecewise affine function of the form

$$\phi = \begin{cases} H^+y + E^+ & \text{if } \sigma(y) > 0 \\ H^-y + E^- & \text{if } \sigma(y) < 0 \end{cases} \quad (13)$$

with  $H^\pm \in \mathbb{R}^{m \times p}$ ,  $E^\pm \in \mathbb{R}^m$  and  $\sigma : \mathbb{R}^p \mapsto \mathbb{R}$  being the linear scalar function

$$\sigma(y) = Sy + s_0$$

where  $S \in \mathbb{R}^{1 \times p}$  and  $s_0 \in \mathbb{R}$ . Here, without loss of generality, we assume that  $S \neq 0$  and  $s_0 = 0$ .

The resulting system is in the form given by (1) where

$$\begin{aligned} F^+ &= (A - BH^+C)x - BE^+, & \text{if } SCx > 0 \\ F^- &= (A - BH^-C)x - BE^-, & \text{if } SCx < 0 \end{aligned} \quad (14)$$

and the switching manifold  $\Sigma$  is defined as

$$\Sigma := \{x \in \mathbb{R}^3 : SCx = 0\}.$$

In the following subsections we consider first the SISO case (case I) where  $C = (1 \ 0 \ 0)$  without loss of generality (corresponding to the classical Lur'e problem), and show that two-fold singularities do not occur. Thereafter we consider more general cases where two-fold singularities can occur and derive the necessary conditions. These include a multiple output system where  $C$  is a general rectangular matrix (case II), and full state feedback where  $C$  is the identity matrix (case III). An interesting special case is a two-dimensional output where the feedback depends on the output  $y$  and its integral.

#### 4.1 Case I. SISO

In this case, the output  $y = Cx$  is a scalar. It is easy to show that no two-fold singularity is possible because the two lines where the vector fields are tangent to the switching manifold  $\Sigma$  are always parallel (Figure 2(left)). Let us demonstrate this with the condition (3) for this simple case, using more geometrically explicit notation.

The condition  $\det(T) \neq 0$  states that the two tangency lines of  $F^\pm$  on  $\Sigma$  are transverse. The tangency lines are where  $\sigma_x F^+ = 0$  and  $\sigma_x F^- = 0$  on  $\sigma = 0$ , *i.e.* the solutions of  $\sigma_x(F_x^\pm x - BE^\pm) = 0$ . Since  $T$  is a  $3 \times 3$  matrix we have that  $\det(X, Y, Z) = X \cdot (Y \times Z)$  in terms of the scalar triple product for general vectors  $X, Y, Z$ . In this case

$$\begin{aligned} \det(T) &= \sigma_x \cdot (\sigma_x F_x^+ \times \sigma_x F_x^-) \\ &= SC \cdot (SCA - SCBH^+C) \times (SCA - SCBH^-C) \\ &= SC \cdot SCA \times (SCBH^+C - SCBH^-C) \end{aligned} \quad (15)$$

where the second line follows from (14) and the last line comes from multiplying out the cross product. That the cross product does not vanish implies the nullcline planes  $\sigma_x F^+$  and  $\sigma_x F^-$

are not coplanar, so their intersections with  $\sigma = 0$  should be two distinct lines. However, the quantities  $S, H$  and  $CB$  are scalars, so we have

$$\det(T) = [S^3 CB(H^+ - H^-)] C \cdot CA \times C \quad (16)$$

Clearly  $C \cdot (CA \times C) = CA \cdot (C \times C) = 0$ , meaning that the two tangency lines are parallel as illustrated in Figure 2(left), and giving  $\det(T) = 0$ .

This violates the condition for two-fold singularities, and therefore might explain why the Teixeira singularity has never been observed in the classical literature on switched control systems, where the typical models are of the single-output system type investigated in this section.

## 4.2 Case II. MIMO

In the most general case, the system is characterised by  $p$  outputs and  $m$  inputs. In this case  $C$  is a  $p \times 3$  matrix and  $S$  is a  $1 \times p$  matrix and the matrix  $T$  in (3) is the  $3 \times 3$  matrix:

$$T = \begin{pmatrix} SC(A - BH^+C) \\ SC(A - BH^-C) \\ SC \end{pmatrix}, \quad (17)$$

which, unlike the single output case, it is not generally singular, so Teixeira singularities will occur generically.

**Remark 1** *Note that the multiple output case includes switched state-feedback control. In this case the output matrix  $C$  is the  $3 \times 3$  identity matrix so the full state is available for feedback, i.e.  $y = x$ . Consequently, the tangency lines are solutions of the equations*

$$Sx = 0, \quad (18)$$

$$S(Ax - BH^\pm x - BE^\pm) = 0. \quad (19)$$

*The Jacobian is simply  $J^\pm = A - BH^\pm$  and the transversely condition in (3) becomes*

$$\det(SJ^+, SJ^-, S)^T \neq 0.$$

**Remark 2** *An interesting special case is that of a two-dimensional linear plant with a dynamic scalar output feedback. Specifically, this is the case where  $\dot{\tilde{x}} = \tilde{A}\tilde{x} + \tilde{B}u$  with  $\tilde{x} \in R^2$  is a planar linear system and the feedback function is set to be*

$$\phi = \begin{cases} \alpha_1^+ \tilde{y} + \alpha_2^+ (\int \tilde{y}) & \text{if } \beta_1 \tilde{y} + \beta_2 (\int \tilde{y}) > 0 \\ \alpha_1^- \tilde{y} + \alpha_2^- (\int \tilde{y}) & \text{if } \beta_1 \tilde{y} + \beta_2 (\int \tilde{y}) < 0. \end{cases} \quad (20)$$

*with  $\tilde{y}$  being a scalar output, say  $\tilde{y} = \tilde{C}\tilde{x}$ .*

It is easy to show that this system can be recast as the general system with multiple outputs. Namely, we extend the state vector by defining  $x = (\tilde{x}^T, \int \tilde{y})^T$ . Then, we choose the matrices in (12) as:

$$A = \begin{pmatrix} \tilde{A} & 0 \\ \tilde{C} & 0 \end{pmatrix}, \quad B = \begin{pmatrix} \tilde{B} \\ 0 \end{pmatrix}, \quad C = \begin{pmatrix} \tilde{C} & 0 \\ 0 & 1 \end{pmatrix}, \quad (21)$$

and those in (13) as

$$H^\pm = (\alpha_1^\pm \quad \alpha_2^\pm), \quad E^\pm = 0$$

with  $\sigma(y) = (\beta_1 \ \beta_2) y$ .

The dynamics close to the singularity can be analysed using the results presented in Section 3, as will be illustrated next by means of a representative example.

## 5 Examples

Here we give three abstract examples that demonstrate the range of behaviour predicted by the analysis above, followed by a model of a PID controller that exhibits a Teixeira singularity for physically viable parameter values.

### 5.1 SISO, SIMO, and MIMO

Consider, as a first example, a SISO system described by the following matrices

$$A = \begin{pmatrix} -1 & 1 & 0 \\ -1 & 0 & 1 \\ -1 & 0 & 0 \end{pmatrix}, \quad B = \begin{pmatrix} 1 \\ 0 \\ 0 \end{pmatrix}, \quad C = (1 \ 0 \ 0),$$

$$H^+ = -1, \quad H^- = 1, \quad E^+ = 1, \quad E^- = -2, \quad S = 1.$$

The switching manifold  $\Sigma$  has equation  $SCx = 0$ , which in this case is equal to  $x_1 = 0$ , and the components of  $F^+$  and  $F^-$  normal to  $\Sigma$  at  $x_1 = 0$  are respectively  $x_2 - 1$  and  $x_2 + 2$ . Equating these to zero gives the tangency lines which are, as expected, parallel. An orbit of this system is depicted in Figure 5.

Next consider the same system with an additional output. We keep all matrices unchanged except for  $B$ ,  $C$  and  $S$  which become

$$B = \begin{pmatrix} 1 \\ 0 \\ -4 \end{pmatrix}, \quad C = \begin{pmatrix} 1 & 0 & 0 \\ 0 & 0 & 1 \end{pmatrix}, \quad S = (1 \ 0). \quad (22)$$

The switching manifold is again the surface  $x_1 = 0$ , but the tangency lines now intersect at the point  $x = (0 \ -1/2 \ 3/2)^T$ . With a little algebra one can show that, independently of the particular choice of the system's matrices, the vector fields  $F^\pm$  at the singularity are equal to

$$\hat{F}^\pm = A\hat{x} - B \left( \frac{SCA\hat{x}}{SCB} \right),$$

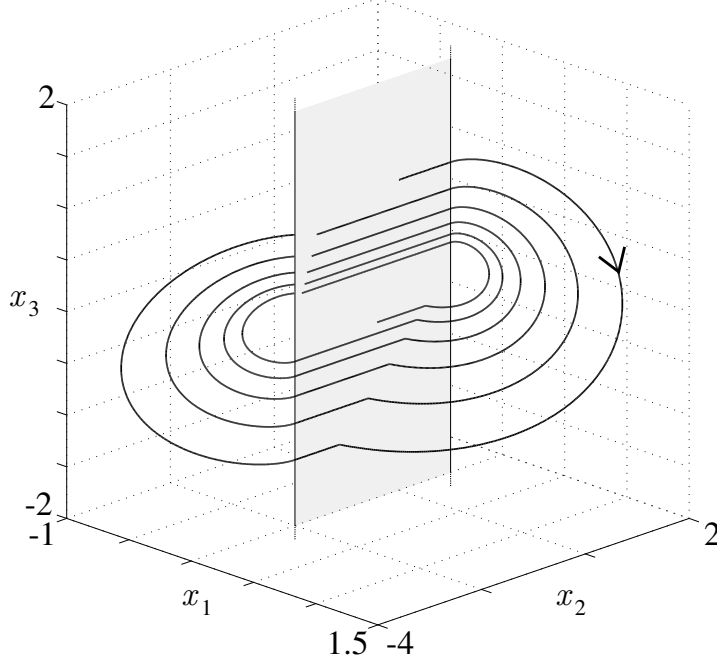


Figure 5: An orbit of the SISO system. The shaded surface is the sliding region  $\Sigma^s$  with parallel boundaries.

that is, they coincide. Hence, a SIMO control scheme can exhibit a Teixeira singularity but, in that case,  $vw = 1$ ,  $v, w > 0$ , for all choices of parameters. This implies that all orbits starting near the singularity (except those starting in the escaping region which is, however, a set of codimension one with respect to the state space) are repelled from it. For the choice of parameters in (22), for example, the point  $\hat{x}$  is a Teixeira singularity, and neighbouring orbits are plotted in Figure 6.

Now consider the same system with an additional input. We keep the same matrix  $A$ , while the other matrices become

$$B = \begin{pmatrix} 1 & 0 \\ 0 & 1 \\ b_{31} & 0 \end{pmatrix}, C = \begin{pmatrix} 1 & 0 & 0 \\ 0 & 0 & 1 \end{pmatrix},$$

$$H^+ = \begin{pmatrix} 0 & -1 \\ 0 & 0 \end{pmatrix}, H^- = \begin{pmatrix} 0 & 1 \\ 0 & 0 \end{pmatrix}, E^+ = \begin{pmatrix} 1 \\ 2 \end{pmatrix}, E^- = \begin{pmatrix} -2 \\ -4 \end{pmatrix}, S = (1 \ 0).$$

We observe the system near the singularity for different values of parameter  $b_{31}$  around 0. The switching manifold is again the surface  $x_1 = 0$ , but the tangency lines now intersect at the point  $x = (0 \ -1/2 \ 3/2)^T$ . At the singularity, the vector field on the two sides of the switching

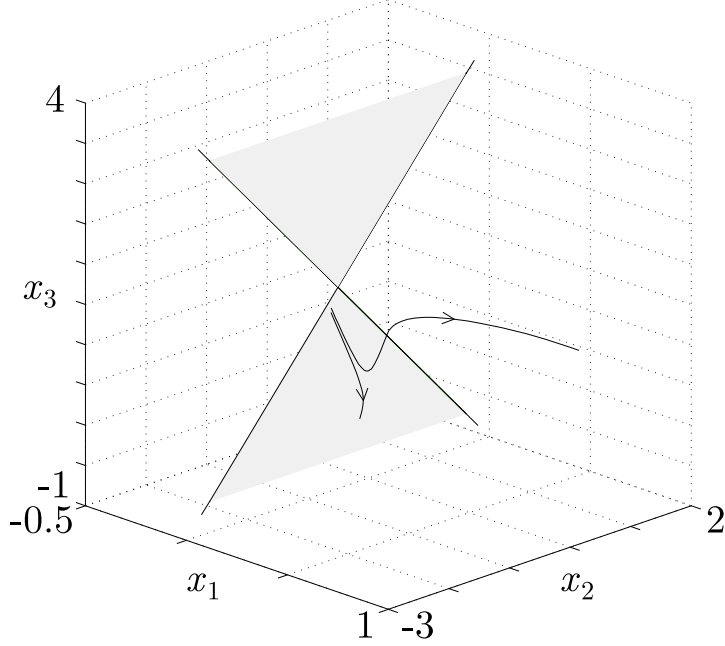


Figure 6: Orbits of the SIMO system. The vector fields  $F^\pm$  coincide at the singularity and, as a consequence, nearby orbits are pushed away from it.

manifold is

$$\hat{F}^+ = \begin{pmatrix} 0 \\ -\frac{1}{2} \\ \frac{b_{13}}{2} \end{pmatrix}, \hat{F}^- = \begin{pmatrix} 0 \\ \frac{11}{2} \\ \frac{b_{13}}{2} \end{pmatrix},$$

thus  $\hat{F}^+$  and  $\hat{F}^-$  are antiparallel when  $b_{13} = 0$ , which corresponds to  $vw = 1$ ,  $v, w < 0$ , the bifurcation introduced in Section 3. In Figure 7a we have  $vw \simeq 0.98$ , which implies that orbits near the singularity reach the sliding region after crossing the switching manifold a finite number of times. The product  $vw$  is approximately equal to 1.1 in Figure 7b and 1.5 in Figure 7c, implying that orbits near the singularity may cross the switching manifold an infinite number of times. With the choice of parameters in this example, a stable limit cycle emerges from the singularity as  $b_{31}$  crosses zero.

At the same time, when the cycle exists, orbits starting close enough to the sliding region (hence in an open subset of the state space!) all converge to the singularity in finite time (since  $vw > 1$  and  $v, w < 0$ ), and are reinjected into the escaping region. Since the vector field at the singularity is not uniquely defined, the evolution of the system after this point is undetermined. This is depicted in Figure 8, where two orbits with different initial conditions are plotted with parameters as in Figure 7c: the black one converges to the limit cycle, while the grey one falls on the sliding region, and reaches the singularity at  $t = \hat{t}$ .

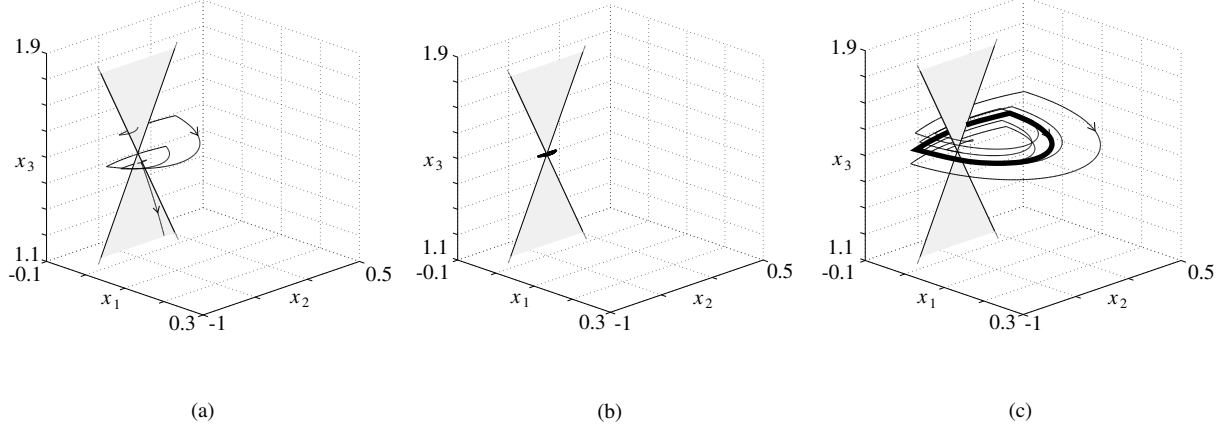


Figure 7: Orbits of the MIMO system for  $b_{31} = -0.01$  (a),  $b_{31} = 0.05$  (b), and  $b_{31} = 0.2$  (c). The upper grey triangle is the escaping region  $\Sigma^e$  and the lower grey triangle is the sliding region  $\Sigma^s$ . The crossing regions are not depicted. The thick curves in (b) and (c) are stable limit cycles.

## 5.2 A PID controller

The model depicted in Figure 9 is derived from a proportional-integral-derivative (PID) controller proposed in [17] (see also [29]). There, a variable structure (switching) PID controller was introduced to prevent integrator windup, which can cause significant loss of performance when used in systems with actuator saturation. The system consists of: a second order plant  $G_p$  controlled through a PID controller, an actuator which saturates the control input from above, and an anti-windup feedback loop.

The system can be modeled by a piecewise-linear ordinary differential equation in  $\mathbb{R}^3$ , given by

$$\dot{x} = \begin{cases} F^+ & \text{if } \sigma(x) > 0, \\ F^- & \text{if } \sigma(x) < 0, \end{cases} \quad (23)$$

where  $x = (x_1, x_2, x_3)^T$  and

$$F^+(x) = \begin{pmatrix} x_2 \\ -a_1x_1 - a_2x_2 + u_{sat} - \sigma(x) \\ x_{1d} - x_1 \end{pmatrix}, \quad F^-(x) = \begin{pmatrix} x_2 \\ -a_1x_1 - a_2x_2 + u_{sat} \\ \rho\sigma(x) \end{pmatrix}. \quad (24)$$

The switching function is given by

$$\sigma(x) = u_{sat} - k_p(x_{1d} - x_1) + k_d x_2 - k_i x_3. \quad (25)$$

This changes sign when the control input passes the saturation value  $u_{sat}$ . As depicted in Figure 9, the error  $(x_{1d} - x_1)$  is multiplied by a constant  $k_p$ , it is derived and the result multiplied by  $k_d$ . Then this is integrated and multiplied by  $k_i$ . When the control input is not saturated ( $\sigma > 0$ ) the saturator behaves like the identity function. Otherwise ( $\sigma < 0$ ) the saturator output is  $u_{sat}$ .

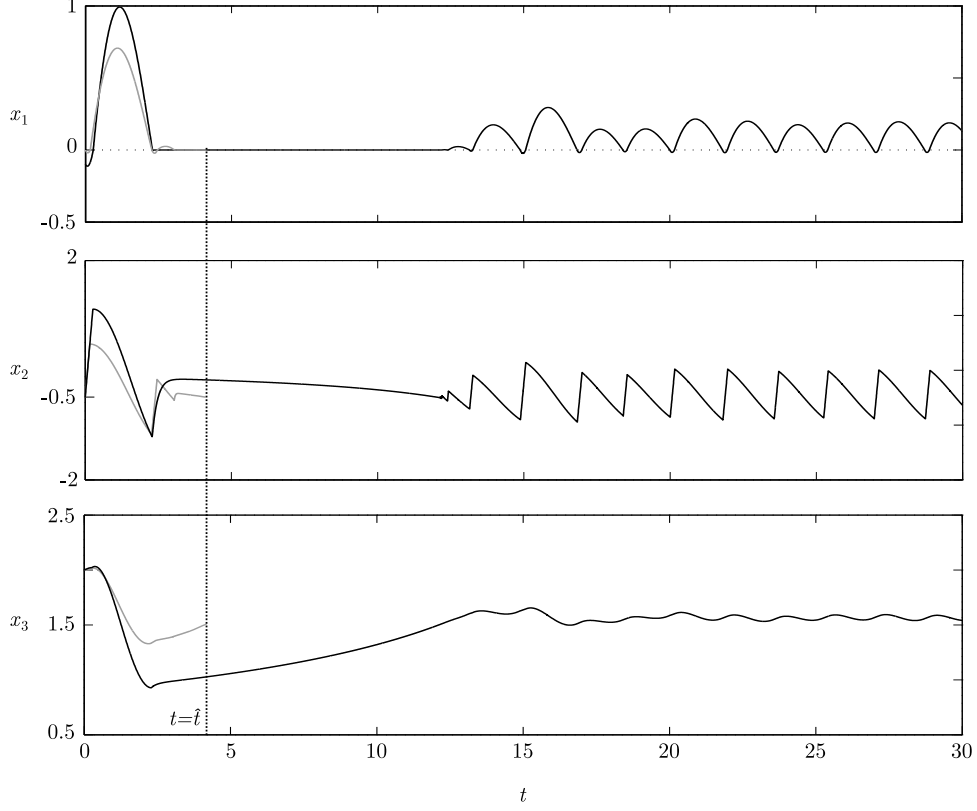


Figure 8: Two orbits of the MIMO system with parameters as in Figure 7c, which has a Teixeira singularity at  $x = (0, -0.5, 1.5)^T$ . The black orbit converges to the limit cycle, while the grey one slides and reaches the singularity at  $t = \hat{t}$ . After this point, the evolution of the system is not uniquely defined.

Then the anti-windup feedback loop is active, and instead of integrating the error we integrate  $\rho\sigma(x)$ .

The two lines of folds, where  $\dot{x}$  is tangent to the switching manifold, are given by

$$\sigma(x) = 0 \quad \& \quad k_p x_2 - k_d (a_1 x_1 + a_2 x_2 - u_{sat}) - k_i (x_{1d} - x_1) = 0, \quad (26)$$

$$\text{and } \sigma(x) = 0 \quad \& \quad k_p x_2 - k_d (a_1 x_1 + a_2 x_2 - u_{sat}) = 0. \quad (27)$$

These cross at the point

$$\hat{x} = \left\{ x_{1d}, k_d \frac{u_{sat} - a_1 x_{1d}}{a_2 k_d - k_p}, \frac{u_{sat}}{k_i} + \frac{k_d^2 (u_{sat} - a_1 x_{1d})}{k_i (a_2 k_d - k_p)} \right\}. \quad (28)$$

To verify that  $\hat{x}$  is a Teixeira singularity we must show:

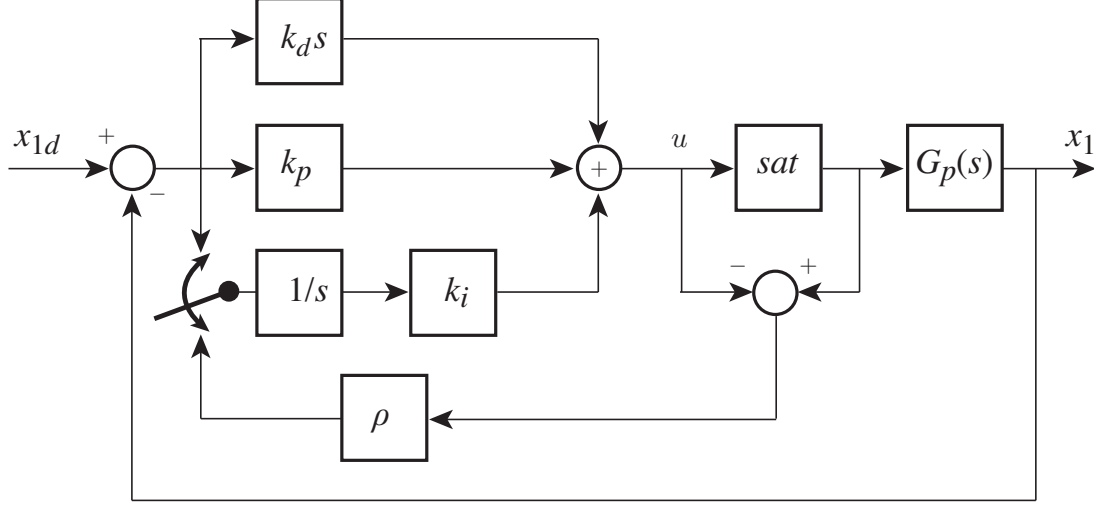


Figure 9: Block diagram of variable structure PID controller.

1. singularity type: the folds are both invisible (Figure 3.1) if

$$\begin{aligned} 0 &> \sigma_x \hat{F}_x^+ \hat{F}^+ = \frac{x_{1d}a_1 - u_{sat}}{a_2k_d - k_p} (k_d^2a_1 + k_p^2 - a_2k_pk_d - k_ik_d) \\ 0 &< \sigma_x \hat{F}_x^- \hat{F}^- = \frac{x_{1d}a_1 - u_{sat}}{a_2k_d - k_p} (k_d^2a_1 + k_p^2 - a_2k_pk_d) \end{aligned}$$

2. nondegeneracy: the folds cross transversally. This holds if  $\det T \neq 0$ , or, from (26-27), simply if  $k_i \neq 0$ .

An example of a parameter range where these conditions are satisfied is:

$$\begin{aligned} k_p &= -11.5 + 3k, & k_d &= -3.25 + k, & k_i &= -3.25 + 2k, & k &\in [4.1, 10], \\ \rho &\in [0.1, 0.5], & u_{sat} &\in [0, 10), & (a_1, a_2) &= (10, 6), & x_{1d} &= 1. \end{aligned}$$

The system this defines is stable (as is easily checked, for instance by plotting the first column of the Routh-Hurwitz scheme). In this, as in many examples we considered, it is found that the product  $vw$  equals unity (for all choices of parameter values). The parameters listed above also give  $v, w > 0$ . The classification in Section 3 reveals that trajectories local to the Teixeira singularity at  $\hat{x}$  can cross the switching manifold only a finite number of times before sliding, and then will flow away from the singularity, giving qualitatively the scenario shown in Figure 7(a). For these parameters, only orbits in the escaping region are able to reach the singularity.

## 6 Conclusions

We have discussed the occurrence of the Teixeira singularity in discontinuous control systems. After introducing analytical conditions to study the existence of such two-fold singularities in



systems of interest, we gave a classification of the dynamics nearby. We then asked why such a singular point has not been frequently detected in the literature on classical nonsmooth control systems in the Lur'e form. We found that indeed the singularity is only present in MIMO systems of this type. Thus classical relay systems, for example, do not exhibit this phenomenon. We then used a representative example to illustrate the possible scenarios when a Teixeira singularity does occur. We saw that its occurrence can give rise to a stable limit cycle and, more notably, to orbits leading to the singular point itself. After reaching this point the orbits are undetermined because the vector field at the singularity is not uniquely defined. Finally we showed an example from the literature where a Teixeira singularity occurred in a design problem.

From the synthesis viewpoint, our analysis indicates that it is important to properly account for the presence of possible Teixeira singularities in closed-loop systems. Indeed, their presence must be avoided, particularly if the control objective is the stabilisation of some equilibrium of interest. At the same time, our results show that inducing a Teixeira singularity in the closed loop system might be a powerful mechanism to produce and control stable limit cycles. The problem in this case is that of properly characterising the region of asymptotic stability of the cycle which, as shown by some preliminary results, can have a complex geometry.

The issue of forward-time non-uniqueness in Filippov systems is well known but often overlooked, because it affects only trajectories in the escaping region, which is locally repelling. The fact that a two-fold allows trajectories from the attractive sliding region to access these forward-time ambiguities, leading to nondeterminism, corresponds to an enormous sensitivity on initial conditions in real physical systems that can no longer be ignored. The Teixeira singularity is one particular example of the resultant behaviour, and further understanding of its occurrence in real applications promises to contribute both to the design of robust efficient controllers, and to the evolving theory of nonsmooth dynamical systems.

Ongoing work is aimed at understanding the role of nonlinearities as we move away from the singularity, and at generalising the analysis presented in this paper to higher dimensional control systems, where a proper theory of Teixeira singularities is completely lacking.

## 7 Acknowledgements

The authors wish to acknowledge useful discussions with M. A. Teixeira during the BCANM workshop on “Problems in Nonsmooth Systems” at the University of Bristol, November 2008. MdB and MRJ acknowledge support from the EPSRC.

## References

- [1] F. Bizzarri, M. Storace, and A. Colombo. Bifurcation analysis of an impact model for forest fire prediction. *Int. J. Bifurcat. Chaos*, 18:2275–2288, 2008.
- [2] B. Brogliato. *Nonsmooth Mechanics - Models, Dynamics and Control*. Springer-Verlag, London, 1999.

- [3] B. Brogliato. *Impacts in Mechanical Systems - Analysis and Modelling*, volume 551 of *Lecture Notes in Physics*. Springer-Verlag, New York, 2000.
- [4] D. R. J. Chillingworth. Discontinuity geometry for an impact oscillator. *Dynam. Syst.*, 17(4):389–420, 2002.
- [5] A. Colombo, M. di Bernardo, S. J. Hogan, and P. Kowalczyk. Complex dynamics in a hysteretic relay feedback system with delay. *J. Nonlinear Sci.*, 17:85–108, 2007.
- [6] A. Colombo, P. Lamiani, L. Benadero, and M. di Bernardo. Two-parameter bifurcation analysis of the buck converter. *SIAM J. Appl. Dyn. Syst.*, 8:1507–1522, 2009.
- [7] H. Dankowicz and X. Zhao. Local analysis of co-dimension-one and co-dimension-two grazing bifurcations in impact microactuators. *Physica D*, 202:238–257, 2005.
- [8] H. de Jong, J.-L. Gouzé, C. Hernandez, M. Page, T. Sari, and J. Geiselmann. Qualitative simulation of genetic regulatory networks using piecewise-linear models. *Bull. Math. Biol.*, 66:301–340, 2004.
- [9] F. Dercole. Border collision bifurcations in the evolution of mutualistic interactions. *Int. J. Bifurcat. Chaos*, 15:2179–2190, 2005.
- [10] F. Dercole, A. Gragnani, and S. Rinaldi. Bifurcation analysis of piecewise smooth ecological models. *Theor. Popul. Biol.*, 72:197–213, 2007.
- [11] M. di Bernardo, C. J. Budd, A. R. Champneys, and P. Kowalczyk. *Piecewise-smooth Dynamical Systems: Theory and Applications*. Springer-Verlag, 2008.
- [12] D. D. Dixon. Piecewise deterministic dynamics from the application of noise to singular equation of motion. *J. Phys A: Math. Gen.*, 28:5539–5551, 1995.
- [13] A. F. Filippov. *Differential Equations with Discontinuous Righthand Sides*. Kluwer Academic Publishers, Dordrecht, 1988.
- [14] J.-L. Gouzé and T. Sari. A class of piecewise-linear differential equations arising in biological models. *Dynam. Syst.*, 17:229–316, 2003.
- [15] F. Grogard, H. de Jong, and J. l Gouzé. *Piecewise-linear models of genetic regulatory networks: Theory and example*. Springer-Verlag, 2007.
- [16] J. P. Hespanha and A. S. Morse. Switching between stabilizing controllers. *Automatica*, 38:1905–1917, 2002.
- [17] A. S. Hodel and C. E. Hall. Variable-structure PID control to prevent integrator windup. *IEEE Transactions on Industrial Electronics*, 48:2,442–451, 2001.
- [18] M. R. Jeffrey and A. Colombo. The two-fold singularity of discontinuous vector fields. *SIAM J. Appl. Dyn. Syst.*, 8:624–640, 2009.
- [19] V. Křivan. Optimal foraging and predator-prey dynamics. *Theor. Popul. Biol.*, 49:265–290, 1996.

- [20] V. Křivan. Dynamic ideal free distribution: effects of optimal path choice on predator-prey dynamics. *Am. Nat.*, 149:164–178, 1997.
- [21] Yu. A. Kuznetsov, S. Rinaldi, and A. Gragnani. One parameter bifurcations in planar Filippov systems. *Int. J. Bifurcat. Chaos*, 13:2157–2188, 2003.
- [22] D. Liberzon. *Switching Systems and Control*. Birkhauser, Boston, MA, 2003.
- [23] M. A. Teixeira. On topological stability of divergent diagrams of folds. *Math. Z.*, 180:361–371, 1982.
- [24] M. A. Teixeira. Stability conditions for discontinuous vector fields. *J. Differ. Equations*, 88:15–29, 1990.
- [25] M. A. Teixeira. Generic bifurcation of sliding vector fields. *J. Math. Anal. Appl.*, 176:436–457, 1993.
- [26] P. Thota, X. Zhao, and H. Dankowicz. Co-dimension-two grazing bifurcations in single-degree-of-freedom impact oscillators. *J. Comp. Nonlinear Dyn.*, 1:328–335, 2006.
- [27] V. I. Utkin. Variable structure systems with sliding modes. *IEEE T. Automat. Contr.*, 22:212–222, 1977.
- [28] V. I. Utkin. Vss premise in xx century: Evidences of a witness. In X. Yu and J.-X. Xun, editors, *Advances in Variable Structure systems, Analysis, Integration and Applications*, pages 1–34. World Scientific, 2000.
- [29] A. Visioli. *Practical PID control*. Springer-Verlag, 2006.